remote sensing

MDPI

Article

Land Cover Change Detection and Subsistence Farming Dynamics in the Fringes of Mount Elgon National Park, Uganda from 1978–2020

Hosea Opedes [1,2,*], Sander Mücher [3], Jantiene E. M. Baartman [1], Shafiq Nedala [2] and Frank Mugagga [2]

[1] Soil Physics and Land Management Group, Wageningen University, 6708 PB Wageningen, The Netherlands; jantiene.baartman@wur.nl
[2] Department of Geography, Geo-Informatics and Climatic Sciences, Makerere University, Kampala P.O. Box 7062, Uganda; shafiq.nedala@students.mak.ac.ug (S.N.); frank.mugagga@mak.ac.ug (F.M.)
[3] Wageningen Environmental Research, Wageningen University & Research, 6708 PB Wageningen, The Netherlands; sander.mucher@wur.nl
* Correspondence: hosea.opedes@wur.nl; Tel.: +256-785-176-128

Abstract: Analyzing the dominant forms and extent of land cover changes in the Mount Elgon region is important for tracking conservation efforts and sustainable land management. Mount Elgon's rugged terrain limits the monitoring of these changes over large areas. This study used multitemporal satellite imagery to analyze and quantify the land cover changes in the upper Manafwa watershed of Mount Elgon, for 42 years covering an area of 320 km^2. The study employed remote sensing techniques, geographic information systems, and software to map land cover changes over four decades (1978, 1988, 2001, 2010, and 2020). The maximum likelihood classifier and post-classification comparison technique were used in land cover classification and change detection analysis. The results showed a positive percentage change (gain) in planted forest (3966%), built-up (890%), agriculture (186%), and tropical high forest low-stocked (119%) and a negative percentage change (loss) in shrubs (−81%), bushland (−68%), tropical high forest well-stocked (−50%), grassland (−44%), and bare and sparsely vegetated surfaces (−14%) in the period of 1978–2020. The observed changes were concentrated mainly at the peripheries of the Mount Elgon National Park. The increase in population and rising demand for agricultural land were major driving factors. However, regreening as a restoration effort has led to an increase in land area for planted forests, attributed to an improvement in conservation-related activities jointly implemented by the concerned stakeholders and native communities. These findings revealed the spatial and temporal land cover changes in the upper Manafwa watershed. The results could enhance restoration and conservation efforts when coupled with studies on associated drivers of these changes and the use of very-high-resolution remote sensing on areas where encroachment is visible in the park.

Keywords: change detection; nature conservation; encroachment; deforestation; land cover changes (LCCs); Landsat; maximum likelihood classifier; Mount Elgon

Citation: Opedes, H.; Mücher, S.; Baartman, J.E.M.; Nedala, S.; Mugagga, F. Land Cover Change Detection and Subsistence Farming Dynamics in the Fringes of Mount Elgon National Park, Uganda from 1978–2020. *Remote Sens.* **2022**, *14*, 2423. https://doi.org/10.3390/rs14102423

Academic Editor: Elias Symeonakis

Received: 31 March 2022
Accepted: 16 May 2022
Published: 18 May 2022

1. Introduction

Land Cover and Land Use have been used interchangeably. Land Cover refers to the attributes of the Earth's land surface and immediate subsurface (inclusive of biota, soil, topography, surface, and groundwater) together with humans, mainly built-up/artificial surfaces [1,2]. The current activities that occur in the land arising from human activities (such as agriculture, wildlife areas, parks, and grazing land) are the representation of land use [3]. By implication, the land cover is the visual result of the interaction of human activities within the current ecosystems. Land Cover Change (LCC) refers to the representation of the replacement of one land cover type by another in the same space [4]. Changes in land cover are detectable by earth observation technologies [4]. In recent decades, land

cover change analysis has obtained a priority focus in global and regional monitoring studies of fragile ecosystems, especially forests, mountains, and water bodies [5,6]. Natural covers including forests, woodlands, grasslands, marshlands, and water bodies have been reported by several studies to have been either converted or reclaimed into agriculture, bare land, and built-up and/or urbanized centers [7–10].

The causes and driving factors of land use and land cover changes vary. Geist et al. [11] described the strongly interlinked causes of land use/cover changes, clustering them into: biophysical, demographic, economic and technological, and institutional and cultural factors. Specifically, the nature of slopes, elevation, geology, soil, and climatic conditions have also been reported as crucial factors [12–14]. Population growth, expansion of arable land, livestock grazing, and extraction of fuelwood are among the proxy variables [15–18]. Other underlying factors of land cover changes include human-induced bush fires, household behavior, policies, distance to settlements, and road infrastructure [14,16,19].

There are several methods of monitoring land cover changes. Change detection is the process of identifying and detecting differences in the state of a given phenomenon by remotely observing it through time and quantifying temporal effects using multitemporal datasets [20]. Originally, field surveys and the use of available records and maps were performed. However, these conventional techniques proved to be expensive and time-consuming [21] and have been replaced by the use of remote sensing and Geographical Information Systems (GIS). The most used change detection techniques include: on-screen digitization of change [22], multi-temporal composite image change detection [23], vegetation index differencing [24], principal component analysis [25,26], post-classification [27–29], and machine learning classifiers such as Support Vector Machine [30,31].

Mount Elgon in Uganda is designated as a man and biosphere reserve. On the higher altitudes (≈2000 m above sea level), Mount Elgon hosts montane forest and a national park with diverse flora and fauna, whereas human settlements and farmland exist on the lower altitudes (<2000 m above sea level) and on the foot slopes of the mountain [32,33]. Being one of the largest extinct volcanoes with highly fertile and productive soils combined with favorable climatic conditions for agriculture, Mount Elgon is one of the most densely populated rural regions in East Africa [18,34,35]. This has led to continuous encroachment into the national park and clearance of vegetation on fragile steep slopes for subsistence farming and settlements [36,37]. For instance, Manjiya County (in Bududa district) lost 41% of humid primary forest between 2002 and 2019 [38]. In turn, these losses have led to land degradation, frequent manifestation of landslides, and flash floods including casualties among the local community [39,40].

Most studies in and around Mount Elgon have concentrated on forest conservation [37], human activities [41], and natural hazards and disasters, especially landslides and soil erosion [42], disaster drivers and modeling [43], and coping strategies [44]. Land use and land cover change studies in Mount Elgon are limited (e.g., [39,45]). Mugagga et al. [39] analyzed land use changes and the implications thereof for landslide occurrence on critical slopes of Mount Elgon, whereas Mugagga et al. [45] investigated the impact of land use change on carbon stocks and its implications to climate variability in mountain environments. The main aim of this study was (1) to quantify spatial-temporal land cover changes and (2) analyze the patterns of land cover flows in the upper Manafwa watershed, at the slopes of Mount Elgon, Uganda, while focusing on the level of conservation at the proxy of the park boundary on the foot slopes of Mount Elgon, from 1978 to 2020, using multi-temporal Landsat satellite imagery.

2. Materials and Methods

2.1. Study Area

The upper Manafwa catchment is situated on the upper slopes of Mount Elgon between latitudes of 00°56′36″ N and 01°07′19″ N and longitudes of 34°20′38″ E and 34°30′33″ E. Its total area is 320 km^2, covering districts of Bududa, Manafwa, Namisindwa, and Sironko, Eastern Uganda (Figure 1). The watershed experiences extensive loss of forest

cover, coupled with visible forms of land degradation, especially in terms of soil erosion processes and landslides. Moreover, this catchment is a site for the Manafwa watershed restoration project (MWARES), an initiative aimed at promoting sustainable agriculture through building resilience and stimulating stewardship among community members. This formed the basis for selecting this study area, and the output of this study would therefore inform specific actions for the project.

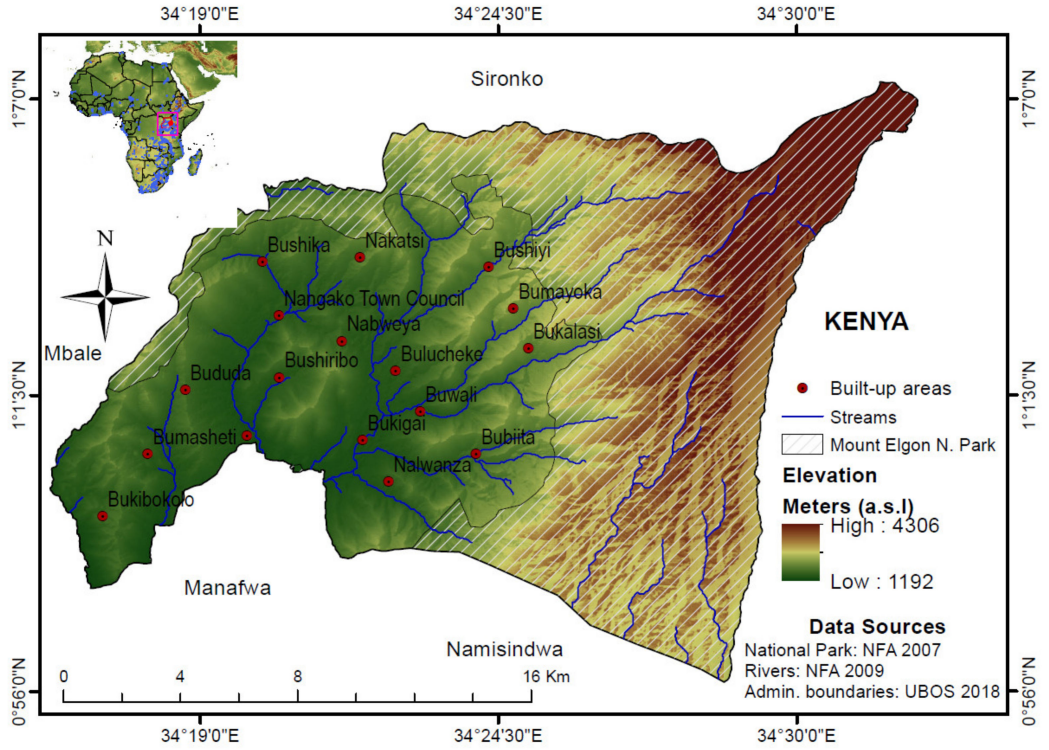

Figure 1. The location and extent of the upper Manafwa watershed with the elevation and drainage system, on Mount Elgon in Eastern Uganda.

Mount Elgon is an extinct volcanic agglomerate of Miocene age that rises up to 4321 m above sea level, located on the Uganda-Kenya border [46]. The study area generally lies at an altitude range between 1800 and 3800 m above sea level [47]. More than 30% of the landscape has steep slopes ranging between 10° and 20°, increasing to steeper than 50° occasionally [48]. The morphology consists of soft thin ash bands that are eroded, forming cliffs of 100–120 m, volcanic cones, interlocking spurs, V-shaped valleys (some with river streams flowing in them), and ridges both gently undulating and rugged [49,50].

The strongly weathered granites of the Basement Complex dominate the geology of the area with a magmatic carbonatite intrusion, biotite granites, and agglomerate lava [51]. Soils are mainly andosols, nitisols, laterite, and vertisols, with a high clay content [40,52]. The soils are relatively young and fertile, being high in calcium, sodium, and potassium [49,53]. The area experiences a bi-modal rainfall pattern of between 1500 mm and 2000 mm per annum and the mean average temperature ranges between 15 °C and 23 °C [45]. These are favorable conditions that attract settlement and intensive farming on the slopes of Mount Elgon (Figure 2). The vegetation on Mount Elgon and the surrounding environment is zoned altitudinally with montane forest types, Afro-Alpine and moorland cover (above 3500 m), heath zone (35,000–3000 m), low canopy and mixed bamboo (3000 m to 2500 m), tropical montane forest (2500 m–1800 m), and the farmlands at the foot slopes [32,45].

Figure 2. Selected photographic view of the land use and land cover in the study area during ground visits to the sample locations: (**a**) agriculture at the periphery of the park, (**b**) built-up and agriculture, (**c**) intensively cultivated slopes with planted forests and landslide scars, and (**d**) the heterogeneity of land cover types and park encroachment.

The major perennial crops grown are arabica coffee (cash crop) and bananas (staple foodstuff). During the rainy season, annual crops (maize, beans, tomatoes, yams, cabbages and onions) are cultivated either as standalone or intercropped with bananas and coffee (Figure 2c,d). The settlements are located on relatively gentle slopes and on ridge tops, as seen in Figure 2b. The study area is among the highly populated areas in Sub Saharan Africa and has a very high annual population growth (3.6%) that exceeds the national average of 3% [18,43]. These demographic characteristics combined with the fact that 40% of the total land area was established as a national park leaves the population with inadequate space for settlement and agriculture [32,54].

2.2. Data Collection and Preparation

A combination of multitemporal Landsat satellite images was used in this study. Figure 3 illustrates the steps followed to achieve study objectives. Five Landsat images, each representing a decade from 1978 to 2020, were acquired from the United States Geological Survey (USGS) Earth explorer website (https://earthexplorer.usgs.gov/ (accessed on 15 December 2020)). Path and Raw of 170/059 and a cloud cover of less than 30% were used in the search criteria. For comparability purposes, images within the dry season (January to March) were acquired, when cloud cover is minimal and the distinction between subsistence agriculture and natural vegetation is much clearer.

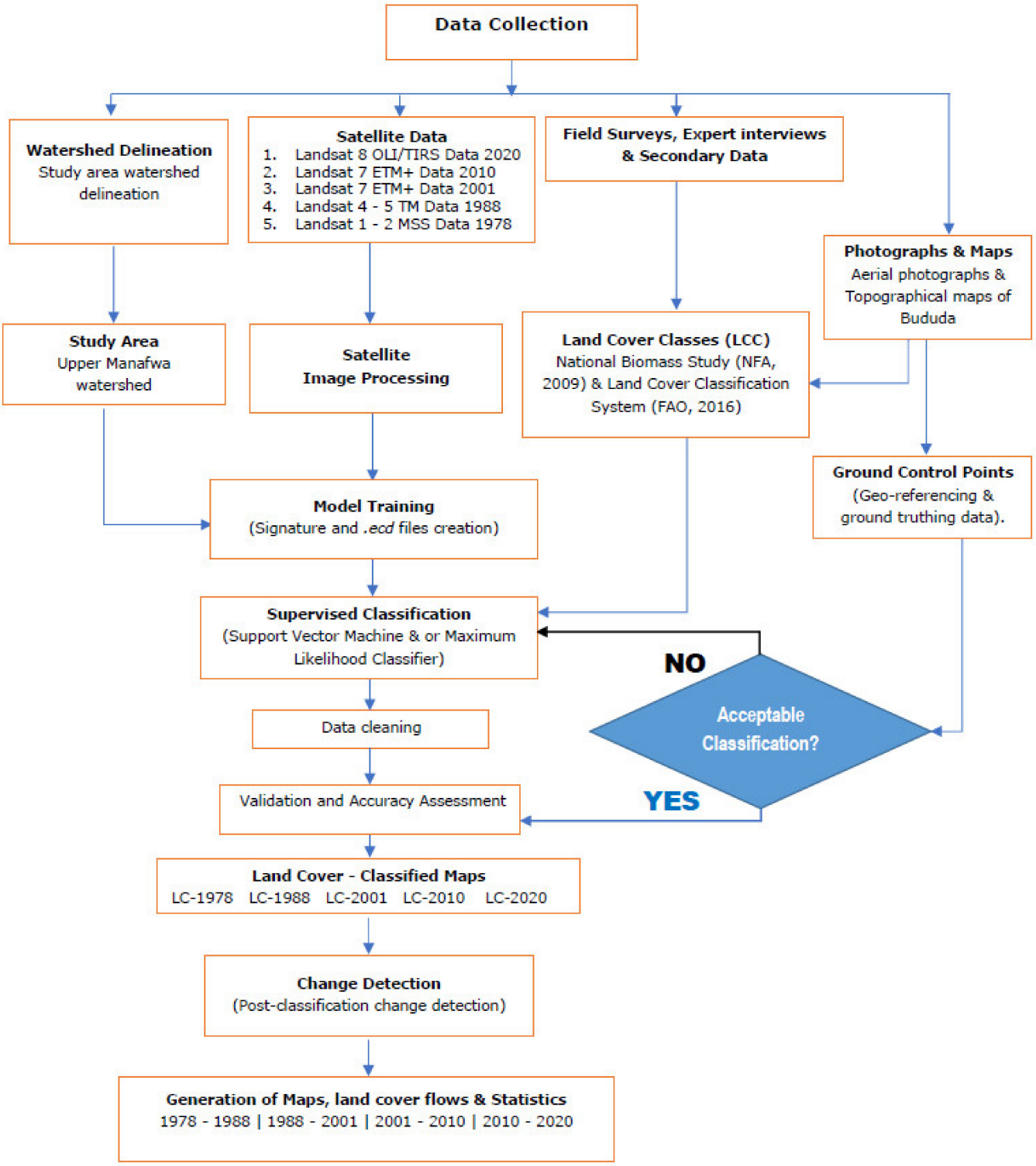

Figure 3. Flow chart for analysis of the land cover change detection in upper Manafwa watershed.

It should be noted that Landsat images of the study area for the specific years 1980 and 1990 could not be found and those of the year 2000 were characterized by high cloud cover. Therefore, images of the most adjacent year (+1 or −1 year to the respective decades) were taken. The satellite imagery considered in this study included: Landsat 8 Operational Land Imager (OLI) and Thermal Infrared Sensor (TIRS) image (for March, 2020); two Landsat 7 Enhanced Thematic Mapper Plus images (for March, 2010 and February, 2001; Landsat 4–5 Thematic Mapper image (for February, 1988); and Landsat 1–2 Multi-Spectral

Scanner (MSS) image (for February, 1978). Particularly, Landsat images were prioritized over other images in this study because of its rich historic database (10 million Landsat scenes) back dating up to 1972 [55]. The images are also medium resolution (30 × 30 m) per pixel [56] and are easily integrated across Landsat missions (1,2,3,5,7,8, and 9). We did not consider replacing Landsat images with sentinel or other satellite images for recent scenes, to avoid temporary misregistration errors due to residual geolocation errors and differences in spectral characteristics with Landsat [57]. The study also considered major changes that could be visible in satellite images after every decade at most.

Ancillary data were acquired for validation, that is, aerial photographs of 1960s and a topographic map of Budadiri (sheet number 54/4) for 1962, at a scale of 1:50,000 from the Department of Surveys and Mapping (see Supplement Figure S1). Field survey and expert interviews were also undertaken in the study area. Ground control points (15) for geometric correction and reference points for ground truthing were collected using TDC600 GPS during field surveys. Training datasets (separate from validation data), averaging 45 training samples per land cover class, were randomly created in the image using visible land cover classes presented in Table 1. Signature files and *.ecd* files were generated for training maximum likelihood and SVM models, respectively. The study adopted the following steps as used in land cover change studies: data collection, image pre-processing and development of classification scheme, training, image classification, ground truthing and accuracy assessment, change detection, and land cover flows (Figure 3). A combination of ArcGIS 10.6.1, QGIS, software packages, and Google Earth Pro was used in various stages of image preparation and analysis for this study.

Table 1. Land Cover Classification scheme used in this study.

Land Cover Class	Description
Built-Up	All built areas and artificially paved surfaces including (rural and urban) residential and service areas, industrial and commercial areas, transportation and communication routes, mine, dump, and construction sites, and green urban/mixed urban
Agriculture	Area of land under seasonal and perennial (food or cash) crop cultivations: mixed farms of bananas, coffee, maize, beans, cabbages, and any other vegetables.
Planted forest	Forests of planted broad-leaved woody trees and/or evergreen needle-shaped leaved trees with top layer trees <65% cover and second layer mixed with coffee and banana plants. Undergrowth of small trees, shrubs, and grasslands with Closed to Open cover of 40–100−40%, respectively.
Bushland	Natural and human-planted vegetation dominated by undergrowth of thickets intermixed with a bunch of grasses growing together as an entity but not exceeding an average height of 4 m.
Grassland	Extensively used grasslands with or without the presence of farm structures such as fences, shelters, enclosures, and watering places
Bare and sparsely vegetated surfaces	Lands with exposed soil and sand, the vegetation cover never exceeds 10% during anytime of the year and stony (5–40%). Includes rock outcrops, bedrock exposures, and accumulation of rock without vegetation, cliffs, and active erosion surfaces.
Shrubs	Mixture of perennial woody shrubs and dotted trees without any defined main stem being less than 5 m tall. The shrub foliage can be either evergreen or deciduous; with or without grass species.
Tropical high forest low-stocked	Degraded or encroached part of the mixed natural forest with indigenous trees, top layer trees less than 20% cover, and second layer mixed with shrubs and bush, consisting of seasonal broadleaf tree communities with an annual cycle of leaf-on and leaf-off periods.
Tropical high forest well-stocked	Primary mixed natural forest with tree canopy >70%, almost all broadleaf trees remain green all year around. Well-stocked and canopy is never without green foliage.

2.3. Image Processing and Classification Scheme

Radiometric and atmospheric correction was performed using the Top of Atmosphere Reflectance (TOA) method, Equation (1) [58]. Landsat tools for Windows Version 1.0.34 software (USGS) 64bits was used to automatically extract variables for radiometric and atmospheric correction from the Meta data file (MTL):

$$P(\infty) = \frac{\pi A,\ (\infty)}{D^{\circ}(\infty) COS\theta} \quad (1)$$

where A = TOA reflectance, D° = solar spectral irradiance that includes Earth–Sun distance correction, and θ = solar zenith angle.

Geometric correction was performed on individual bands through georeferencing the datasets with 15 Ground Control Points (GCPs) of known features validated from the topographic map and in the field. Nine GCPs were spread-out at the edges of the study area and six within the study area. The datasets were then re-projected to EPSG 32636 (https://epsg.io/32636 (accessed on 5 July 2020)). Harmonization of Landsat 1–5 images to Landsat 8 was performed using the resampling technique—Nearest Neighbor Analysis (NNA) in ArcGIS. Finally, composite images for each decade were generated by stacking all bands of Landsat (composite bands tool; ArcGIS). Gap filling was performed in QGIS 3.4.3 using gap mask data as a correction layer in Gap Mask package. The scan line error for Landsat 7 image of 2010 was also corrected (see Figure 4). Image enhancement was performed using histogram equalization and the bilinear interpolation resampling method to improve spectral clarity and visualization.

The Land Cover Classification Scheme (LCCS) for the study was developed in line with the LCCS of the Food and Agricultural Organization (FAO) [59], Anderson et al. [60] and the National Forestry Authority (NFA) [61]. Nine dominant land cover classes were adopted based on physiographic knowledge of the study area (Table 1). The delineated classes were: built-up, agriculture, planted forest, bushland, grassland, bare and sparsely vegetated surfaces, tropical high forest low-stocked, and tropical high forest well-stocked.

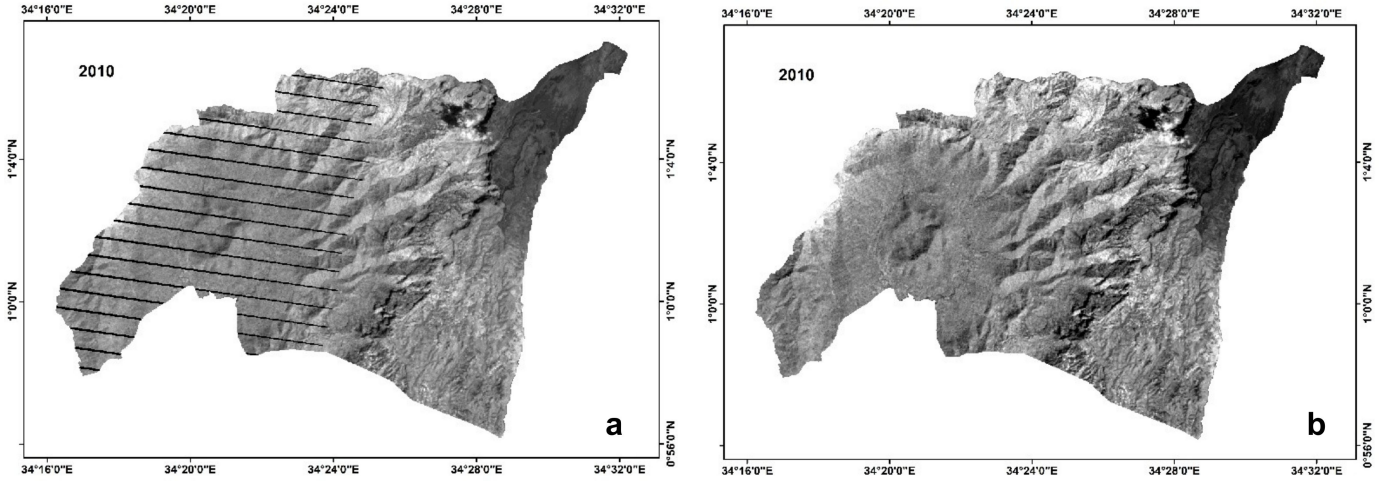

Figure 4. A view of the scan line corrector (SLC) failure of Landsat 7 image acquired in 2010: (**a**) SLC-Off and (**b**) SLC-Off correction.

2.4. Landsat Image Classification and Accuracy Assessment

Several methods for image classification exist [6,62] and each presents its own advantages and disadvantages. In order to choose the most appropriate method for the watershed, a comparative analysis was undertaken between Support Vector Machine (SVM) and supervised classification for one recent satellite image (2020). From the results of accuracy assessment, the Maximum Likelihood (ML) method performed slightly better (90.35%) than SVM (88.46%); thus, ML was used. Furthermore, supervised classification is commonly used because it is simple and quick to implement, allows a clear interpretation of the outcomes, and mostly delivers a satisfactory accuracy [6].

The accuracy of the final change maps was assessed following the recommended best practices and formulae proposed by [63,64]. Using a stratified random sampling technique [64], a total of 387 sample units were generated and distributed appropriately, as illustrated in Table 2 [64]. The same procedure was followed for all other change maps of 2010, 2001, 1988, and 1978. The user's, producer's, and overall accuracy were computed following Equations (2)–(6) [63].

$$W_i = \frac{a}{b} \tag{2}$$

$$P_{rop} = \sum^{3} W_i \frac{a}{b} \quad (3)$$

$$Users = \frac{d_{\circ}}{r} \quad (4)$$

$$Producers = \frac{d_{\circ}}{c} \quad (5)$$

$$Overall = \sum d_{\circ} \quad (6)$$

where a is the number of pixels per strata and b is the total number of pixels in the study area, $d_{\circ}$ is the correctly classified pixels in the diagonal, r is the sum of row pixels, and c is the sum of column pixels.

Table 2. Allocation of sample sites to strata for validation data.

Class	W_i	U_i	Number of Validation Sites
Built-up area	0.049	0.92	25
Agriculture	0.300	0.83	102
Planted forest	0.059	0.92	30
Bushland	0.020	0.88	20
Grassland	0.099	0.95	40
Bare and sparsely vegetated surfaces	0.058	0.68	30
Shrub	0.014	0.76	20
Tropical high forest low-stocked	0.187	1.00	60
Tropical high forest well-stocked	0.213	1.00	60
Total number of validation sites			387

W_i—mapped area proportions, U_i—values of user's accuracies for year = 2020, and column 4 contains the appropriate sample allocation used in this study.

2.5. Change Detection and Land Cover Flows

Change detection analysis was performed using the post-classification comparison (PCC) technique based on supervised classification products [65]. The method involved overlaying independently classified coincident thematic maps and comparing their corresponding classes to determine change transitions starting with the latest year [29,65,66]. In this study, five registered and independently classified images (2020, 2010, 2001, 1988, and 1978) covering four decades (1978–2020) were used to calculate major changes in land cover. Using the back dating approach, the classified 2020 image was used as a reference to classify older images [67]. In order to ensure that the changes are not arising from noise, especially for the older images, the 2020 image was superimposed on older images to identify changes, hence creating respective land cover maps for the older years (2010, 2000, 1988, and 1980). The aerial photographs of 1960s were instrumental in reducing errors especially for the 1978 and 1988 image classification. Equation (7) was used to determine the Magnitude of Change, MoC (km^2):

$$\text{Magnitude of Change, MoC} \left(km^2\right) = \text{Yf} - \text{Yi} \quad (7)$$

where Yi = Class Area (km^2) at the initial year, Yf = Class Area (km^2) at the final year, and n = number of years of the time period.

The classified land cover maps were used to establish the nature of land cover flows between the land cover classes. Land cover flows were established using the raster calcula-

tor function in ArcGIS Pro using Equation (8). The resultant statistics were used to establish land cover flows "from 1978" and "to 2020".

$$\text{Land cover flow } \left(\text{km}^2\right) = (y_1 * (n + 1)) + (y_2) \quad (8)$$

where y_1 = area of all land cover classes of the initial year, y_2 = area of all land cover classes of the final year, and n = number of land cover classes.

3. Results

3.1. Accuracy Assessment of Land Cover Classification

Overall, the classified maps of 2020, 2010, 2001, 1988, and 1978 achieved very high accuracy values of 90%, 89%, 87%, 86%, and 84%, respectively (Table 3).

Table 3. Classification accuracy assessment of the land cover maps obtained from Landsat satellite data at the upper Manafwa watershed for the selected years (2020–1978).

Year	1978		1988		2001		2010		2020	
Land Cover Classes	**UA**	**PA**	**UA**	**PA**	**UA**	**PA**	**UA**	**PA**	**UA**	**PA**
Built-Up	86	79	89	82	78	81	84	85	87	88
Agriculture	69	83	79	97	75	76	78	95	78	95
Planted forest	73	88	92	80	91	86	95	92	96	100
Bushland	79	77	90	75	75	82	83	97	85	97
Grassland	79	80	89	84	83	99	87	88	92	93
Bare and sparsely vegetated surfaces	73	87	94	93	74	74	96	93	100	93
Shrub	91	97	87	75	81	83	92	75	95	84
Tropical high forest low-stocked	68	66	91	95	92	71	100	94	100	94
Tropical high forest well-stocked	76	98	76	99	90	98	93	99	93	100
Overall Accuracy	**84%**		**86%**		**87%**		**89%**		**90%**	

NOTE: UA is User's Accuracy and PA is Producer's Accuracy.

3.2. Land Cover Change from 1978 to 2020

Table 4 illustrates the details of land cover area (km^2 and percentage) for the period from 1978 to 2020. In 1978, tropical high forest well-stocked was the dominant land cover type, covering 139.4 km^2 (43.6%) of the total land area. This cover was followed by grassland 49.7 km^2 (15.6%) and agriculture 34.0 km^2 (10.6%). The lowest land cover in 1978 was planted forest with the cover of 1.6 km^2 (0.5%). The results showed a significant increase of 10.63% and decrease of 13.24% in grassland cover between 1988 and 2001, and 2001 and 2010, respectively. These variations indicate high conversion rates of shrubs to grassland and grassland to agriculture and other classes. Specifically, agriculture increased by 11.10% while shrubs significantly decreased by 5.94% between 2001 and 2010. These changes are attributed to the conservation policy change in Uganda during the same period. The policies and legislation frameworks called for zonation and re-demarcation of the park, which consequently affected enforcement [37,68].

After 1978, land cover changes were visible in 1988, 2001, 2010, and 2020 across all the land cover types, as shown in Figure 5. It is worth noting that the percentage change from 1978 to 2020 was as follows: planted forest (3966%), built-up (890%), agriculture (186%), tropical high forest low-stocked (119%). Furthermore, the negative percentage change was recorded by shrubs (−81%), bushland (−68%), tropical high forest well-stocked (−50%), grassland (−44%), and bare and sparsely vegetated surfaces (−14%) in the period of 1978–2020.

By 2020 when the study ended, agriculture was the dominant land cover type with 30.43% of the total land area (Table 4 and Figure 5). This was followed by tropical high forest well-stocked (21.64%), tropical high forest low-stocked (18.96%), grassland (8.66%), planted forest (5.98%), bare and sparsely vegetated surfaces (5.91%), built-up (4.96%), bushland (2.01%), and shrubs with the lowest cover of 1.46%. Figure 6 illustrates the classified land cover maps for 1978, 1988, 2001, 2010, and 2020 for the upper Manafwa watershed.

Table 4. The area coverage (km^2 and percentage) of different land cover categories in the upper Manafwa watershed during 1978, 1988, 2001, 2010, and 2020.

Land Cover Class	Area (km^2 and %)									
	1978		1988		2001		2010		2020	
	km^2	%	km^2	%	km^2	%	km^2	%	km^2	%
Built-Up	1.60	0.50	2.42	0.76	3.12	0.98	9.60	3.00	15.84	4.96
Agriculture	33.95	10.63	52.69	16.49	56.18	17.58	91.72	28.71	97.22	30.43
Planted forest	0.47	0.15	1.70	0.53	1.57	0.49	3.09	0.97	19.11	5.98
Bushland	20.13	6.30	25.59	8.01	14.72	4.61	19.84	6.21	6.41	2.01
Grassland	49.67	15.55	40.44	12.66	74.39	23.29	32.11	10.05	27.66	8.66
Bare and sparsely vegetated surfaces	22.07	6.91	22.95	7.18	16.37	5.12	25.11	7.86	18.88	5.91
Shrubs	24.52	7.67	12.20	3.82	27.02	8.46	7.69	2.41	4.66	1.46
Tropical high forest low-stocked	27.67	8.66	37.79	11.83	20.64	6.46	50.06	15.67	60.56	18.96
Tropical high forest well-stocked	139.41	43.64	123.69	38.72	105.48	33.02	80.27	25.12	69.13	21.64
Total	319.48	100	319.48	100	319.48	100	319.48	100	319.48	100

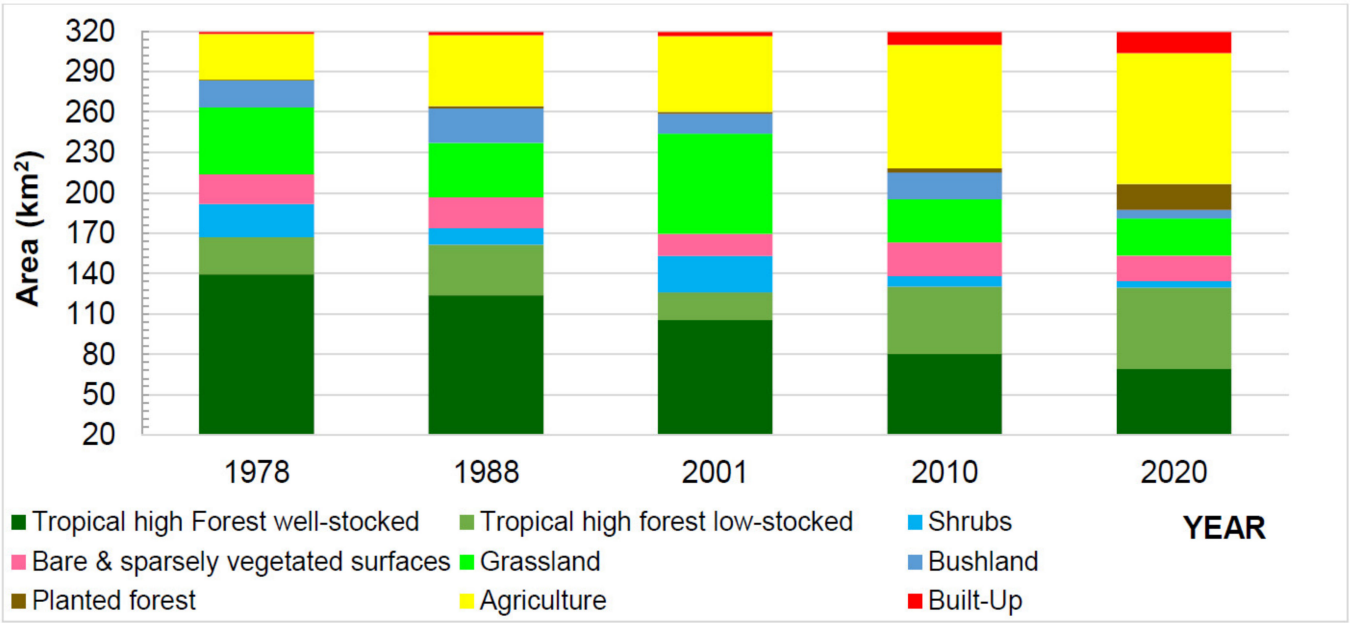

Figure 5. The amount of land cover (km^2) for the period from 1978 to 2020 for the upper Manafwa watershed.

The decadal land cover changes for the period from 1978 to 2020 are well illustrated in Table 5. The land cover change pattern from 1978 to 2020 indicates a general decrease in natural and indigenous vegetation cover. Specifically, tropical high forest well-stocked lost 70.28 km^2, followed by grasslands (22.01 km^2), shrubs (19.86 km^2), bushland (13.72 km^2), and bare and sparsely vegetated surfaces (3.19 km^2). Agriculture recorded the highest land cover gain (63.27 km^2) followed by tropical high forest low-stocked (32.89 km^2), planted forest (18.64 km^2), and built-up (14.24 km^2) in the period from 1978 to 2020. It is worth noting that the tropical high forest low-stocked was the only natural cover class with land cover gain over the time period of 1978–2020 (Table 5). The land cover types supporting human population growth and income-generating activities increased, especially agriculture, planted forest, and built-up areas.

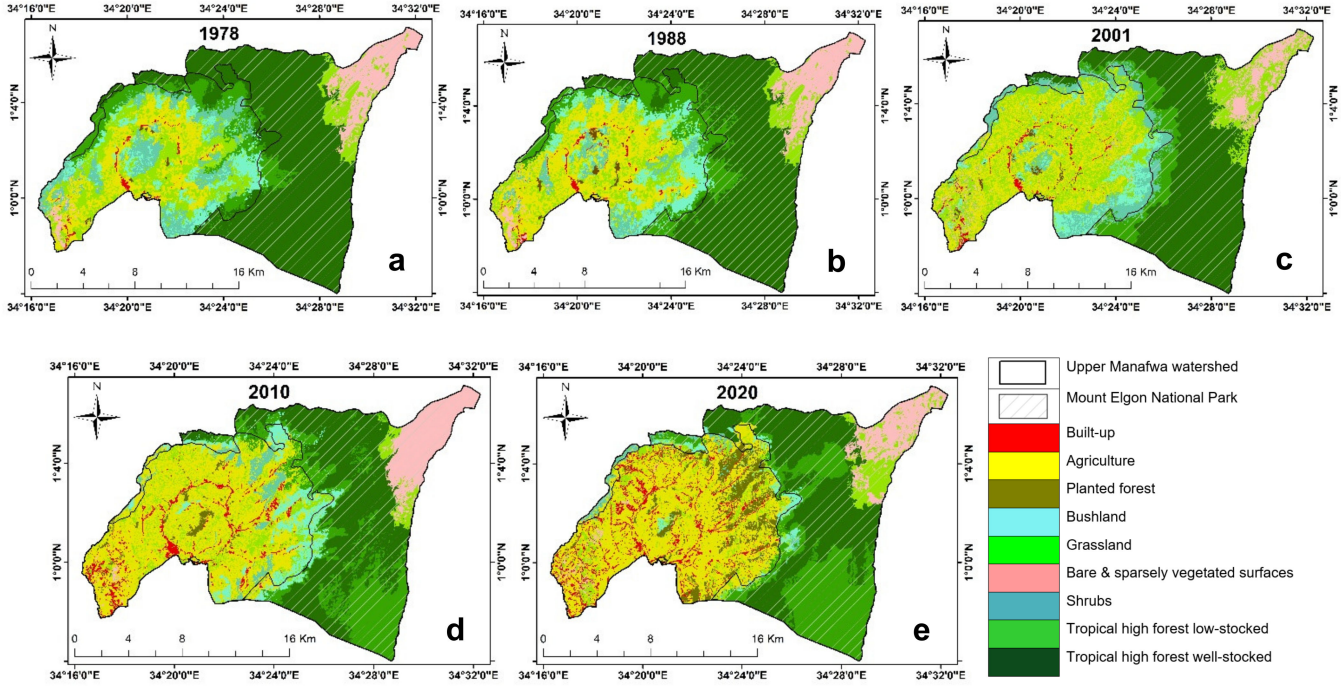

Figure 6. The classified land cover maps for 1978 (**a**), 1988 (**b**), 2001 (**c**), 2010 (**d**), and 2020 (**e**) of upper Manafwa watershed.

Table 5. The decadal land cover changes for the period from 1978 to 2020 showing the area changes in km^2.

Land Cover Class	Status 1978	Area (km^2) 1978–1988	1988–2001	2001–2010	2010–2020	1978–2020	Status 2020
Built-up	1.60	0.82	0.7	6.48	6.24	14.24	15.84
Agriculture	33.95	18.74	3.49	35.54	5.50	63.27	97.22
Planted forest	0.47	1.23	−0.13	1.52	16.02	18.64	19.11
Bushland	20.13	5.46	−10.87	5.12	−13.43	−13.72	6.41
Grassland	49.67	−9.23	33.95	−42.28	−4.45	−22.01	27.66
Bare and sparsely vegetated surfaces	22.07	0.88	−6.58	8.74	−6.23	−3.19	18.88
Shrubs	24.52	−12.32	14.82	−19.33	−3.03	−19.86	4.66
Tropical high forest low-stocked	27.67	10.12	−17.15	29.42	10.50	32.89	60.56
Tropical high forest well-stocked	139.41	−15.72	−18.21	−25.21	−11.14	−70.28	69.13

Note: The negative (−) sign shows decrement in cover between decades.

3.3. Change Detection and Land Cover Flows

Figure 7 shows land cover flows for 1978–1988, 1988–2001, 2001–2010, and 2010–2020. There were a total number of 34, 61, 58, and 63 land cover flows for the years 1978–1988, 1988–2001, 2001–2010, and 2010–2020, respectively. The highest land cover flows (>6) were in shrubs and grassland for 1978–1988; grassland, bushland, agriculture, and tropical high forest low-stocked for 1988–2001; grassland and shrubs for 2001–2010, and tropical high forest well-stocked, tropical high forest low-stocked, grassland, bushland, and agriculture for the period of 2010–2020. These land cover flows amounted to 58.61, 149.16, 145.96, and 132.02 km^2 land cover transitions in between the classes for the years 1978–1988, 1988–2001, 2001–2010, and 2010–2020, respectively. Specifically, the highest transitions (above 15 km^2) included the following: conversion of 15.62 km^2 of tropical high forest well-stocked into tropical high forest low-stocked from 1978 to 1988, and conversion of agriculture area of 20.09 km^2 into grassland in 1988–2001; tropical high forest well-stocked lost 34.59 km^2 to tropical high forest low-stocked, whereas agriculture expanded and gained 26.41 km^2

from grassland between 2001 and 2010, and the outstanding conversions in 2010–2020 were grassland to agriculture (15.64 km^2) and tropical high forest low-stocked to tropical high forest low-stocked (20.34 km^2). It is worth noting that bare and sparsely vegetated surfaces did not experience any conversion in 1978–1988 as compared to other classes during the four years considered by the study.

Figure 7. Land cover flows in years of (**a**) 1978–1988, (**b**) 1988–2001, (**c**) 2001–2010, and (**d**) 2010–2020 for the upper Manafwa watershed. The width of the lines represents the land conversion area (km^2), the number after the label is the start and end years, and the height of the bars represent the size of the land cover class in the start and end years for each decade considered in this study.

Table 6 shows the land cover change flow matrix for the changed areas in their equivalent percentages from 1978 to 2020, in comparison to their total land area. The classes with the highest transitions (>90%) include shrubs with 99.51%, closely followed by bushland (98.26%), planted forest (96.38%), and tropical high forest low-stocked (91.08%). Although tropical high forest well-stocked revealed a 54.51% transition to other classes, it should be noted that 41.20% of it was to tropical high forest low-stocked. Agriculture (27.29%) and bare and sparsely vegetated surfaces (39.03%) revealed the lowest transitions in the same period. From 1978 to 2020, the percentage area of land cover classes that did not change included 72.71% of agricultural area, followed by bare and sparsely vegetated surfaces (60.96%), built-up (46.45%), tropical high forest well-stocked (45.48%), and grassland (13.76%), with the rest below 10% (Table 6). This indicates that natural land cover classes were less persistent and presented more changes, especially shrubs, bushland, and

tropical high forest low-stocked as compared to planted forest, built-up, and agriculture. Furthermore, it is only agriculture that received more than 35% of the transitions from almost all other classes, that is 88.51% from planted forest, 62.85% from grassland, 53.21% from shrubs, 43.28% from tropical high forest low-stocked, and 39.92% from built-up in the period of 1978 to 2020.

Table 6. The land cover change flow matrix (percentage) in the upper Manafwa watershed between 1978 and 2020.

	Class	**Innitial State—1978 (%)**								
		BU	**AG**	**PF**	**BL**	**GL**	**BSVS**	**SH**	**TFLS**	**TFWS**
Final State 2020 (%)	BU	**46.45**	13.63	4.09	7.97	9.4	1.79	6.75	5.26	0.16
	AG	39.92	**72.71**	88.51	62.85	53.54	6.38	53.21	43.28	4.52
	PF	0.83	2.99	**3.61**	15.82	6.80	0.13	25.06	10.52	1.36
	BL	0	0.02	0	**1.74**	0.04	0	1.96	6.86	2.56
	GL	12.11	8.90	3.78	8.27	**13.76**	27.39	5.85	13.63	2.82
	BSVS	0.70	1.74	0	0.08	8.45	**60.96**	1.03	0	0.37
	SH	0	0.01	0	0.32	0.08	0	**0.49**	8.05	1.52
	TFLS	0	0	0	2.95	0.22	0	0.09	**8.92**	41.20
	TFWS	0	0	0	0	7.72	3.34	5.56	3.48	**45.48**
Total Class Change		**100** **53.56**	**100** **27.29**	**100** **96.38**	**100** **98.26**	**100** **86.25**	**100** **39.03**	**100** **99.51**	**100** **91.08**	**100** **54.51**

BU—Built-up, AG—Agriculture, PF—Planted forest, BL—Bushland, GL—Grassland, BSVS—Bare and sparsely vegetated surfaces, SH—Shrubs, TFLS—Tropical high forest low-stocked, TFWS—Tropical high forest well-stocked. **NOTE:** The highlighted diagonal numbers in bold represent the equivalent percentages of land cover proportions that did not change from 1978 to 2020.

Figure 8 illustrates spatially the resultant (final) land cover flows registered in the upper Manafwa watershed in the ranges of 1978–1988, 1988–2001, and 2010–2020 (output of Equation (8)). The park boundary from the National Forestry Authority [69] was overlayed to illustrate the level and impact of land cover flows at the park and community, as shown in Figure 8. Most of the land cover flows occurred at the fringes of the park boundary in 1978–1988 and 1988–2001. Specifically, tropical high forest well stocked was converted into tropical high forest low-stocked in these periods. Inside the park, tropical high forest well-stocked and grassland recorded gains from tropical high forest low-stocked and bare and sparsely vegetated surfaces in 1988–2001 and 2001–2010. Agriculture and grasslands experienced land cover inflows from shrubs and bushland in 1988–2001 and 2001–2010. Interestingly, tropical high forest low-stocked recorded more gains from tropical high forest well-stocked inside the park, and the reverse also occurred in other parts of the park in 2010–2020. However, tropical high forest low-stocked revealed more gains in general from tropical high forest well-stocked, whereas built-up and agriculture revealed more gains outside the park area in 2010–2020. It is worth noting that the outstanding flows were mostly from other land cover types to agriculture and tropical high forest low-stocked, as also seen from the Sankey diagram in Figure 7. These changes were specifically observed in the North East and South Western parts of the study area. The land cover classes of agriculture, built-up, and planted forest have either encroached or threatened to encroach the national park, as seen from the boundary line. These observations are also illustrated in Figure 2a,d, where new farms were established at the proxy of the park after fires in the dry season. Furthermore, napier grass (*pennisetum purpureum*) was also planted within the boundary line. These grasses indirectly replace the natural grassland cover (as napier grass is frequently harvested for the zero grazed animals).

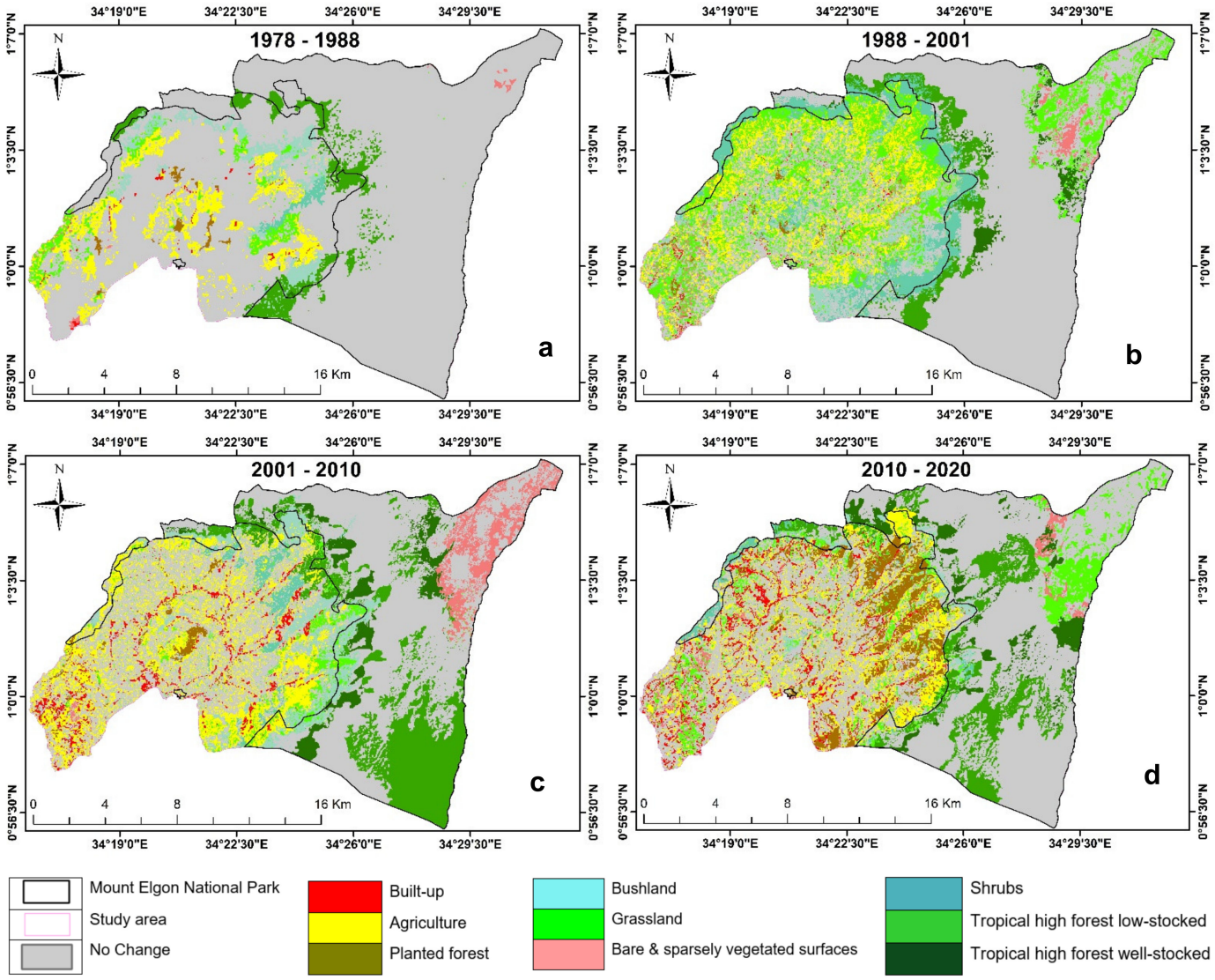

Figure 8. The geospatial distribution of land cover change flows for (**a**) 1978–1988, (**b**) 1988–2001, (**c**) 2001–2010, and (**d**) 2010–2020. The colors represent the "into" (final) land cover gains by each class at end year (1988, 2001, 2010, and 2020). The grey color represents the persistent land cover area (that did not change) in the years 1978, 1988, 2001, 2010, and 2020.

4. Discussion

The results on the accuracy assessment show that the five maps and the nine land cover classes considered by this study were in good agreement and in the excellent accuracy category according to Pontius [70], Sousa et al. [71], and Hailu et al. [72]. The low user's and producer's accuracy for some classes was possibly due to the heterogeneousness and resultant extent of the classes [30]. Nonetheless, results on overall accuracy were above 80%, signifying an acceptable classification accuracy.

The land cover change results from 1978 to 2020 indicate that most of the tropical high forest high-stocked, grassland, shrubs, bushland, and bare and sparsely vegetated surfaces were converted to agriculture, tropical high forest low-stocked, planted forest, and built-up areas. Previous studies in the Mount Elgon region (on both the Kenyan and Ugandan sides) have documented an increasing human pressure on land due to the expansion of settlements and agriculture [68,73]. While this study focused on the upper Manafwa watershed and the national park boundary, the trends found in the current study are in agreement with those observed by previous studies in the broader Mount Elgon region [18,36,39]. Studies elsewhere by Alam et al. [74] (Kashmir Valley, India), Bantider et al. [75] (Wello escarpment,

Burka, Ethiopia), and Liu et al. [76] (Gannan Prefecture, Gansu province, China) also documented the increase in population as a key factor to the expansion of built-up areas that threatened other land cover types [74–76].

The trend of land cover change from 1978 to 2020 in the upper Manafwa watershed highlights the influence of socioeconomic forces on natural land cover conversion. According to previous studies, forest cover on Mount Elgon in general experienced widespread encroachment and deforestation between the 1980s and early 2000s owing to population pressure, political instability, and laxity in the implementation of environmental policies [46,68,77]. Although there were efforts toward curbing deforestation and encroachment, a large stance of tropical high forest well-stocked cover was hence lost into tropical high forest low-stocked, shrubs, bushland, and agricultural land [8,37]. These land cover out-flows arose especially in areas where the community members frequented the park (illegally) to access firewood, bamboo shoots (*maleewa*), medicinal plants, and other forest products [36,37,78]. Over time, the continued access and illegal extraction of some park resources led to the decline in forest cover and, therefore, accelerated land cover changes in the park area [40,46].

Farmland expansion, intensive pasture harvesting from the park for zero grazed animals, and seasonal human-induced fires have reduced grasslands into bare and sparsely vegetated surfaces [68]. The human-induced fires on higher altitudes especially in the park have led to the seasonal occurrence of bare patches on grasslands, shrubs, and bushland during the dry season. These patches have been transformed into farmland in the long run [36,79]. Furthermore, there were conflicts over access, use, and control of the park, combined with political instability and inadequate laws and policies on conservation [46,80]. Enforcement of the law and limited monitoring of the national park also had a significant implication to land cover changes [18]. These conflicts and laxity on conservation area management led to rapid land cover out-flows from well-stocked to low-stocked tropical high forest cover in the 1970s through 1990s. Similar dynamics have been reported elsewhere, for instance, studies in the Ethiopian highlands have also documented the continuous disappearance of forests [5,22] as a result of conflict.

In order to restore heavily degraded landscapes in Mount Elgon, small-scale regreening activities have been undertaken by government agencies, Community-Based Organizations (CBOs), and with the communities [81,82]. These activities combined with tree planting campaigns have led to an increase in planted forest cover within the upper Manafwa watershed (see Figures 2c and 6e). The land cover gains of tropical high forest well-stocked has been attributed to the several recent policy and socioeconomic reforms implemented jointly by the government with adjacent communities to the park [18]. The enactment of laws and policies in the early 2000 that were geared toward conservation, i.e., the National Environment Act cap 153, Forest Policy and the National Environment (Hilly and Mountainous Area Management) Regulations, 2000 played a critical role in streamlining conservation in the Mount Elgon region [37,68].

The contribution of bilateral organizations and regional bodies in the implementation of conservation-related programs and projects have also been instrumental. For instance, the Mount Elgon Regional Ecosystem Conservation Program (MERECP), implemented by the International Union for Conservation of Nature (IUCN) together with the East African Community (EAC), has been documented to have been pivotal in enhancing conservation in the entire Mount Elgon area [83,84]. International conservation organizations have also funded and/or implemented short-term conservation-related projects in the Mount Elgon region such as the World Wide Fund for Nature (WWF) and United Nations Development Program (UNDP) [33,85]. Furthermore, the introduction of several socioeconomic development projects into the community and the use of collaborative conservation approaches have also been echoed to have a positive impacts toward regreening of the park and community landscapes [86,87]. For instance, the Manafwa Watershed Restoration (MWARES) Project trains farmers to become good stewards to their land and sustainably utilize their

natural resources through capacity building on soil and water conservation practices using the Integrated Farm Plan (PIP) approach [87].

In order to take more informed decisions and actions, subsequent studies should thoroughly analyze the drivers of these land cover changes. Integrating biophysical and socioeconomic drivers with these results will further facilitate an understanding of the dynamics of land use and cover changes in the Mount Elgon region and Manafwa watershed in particular. Given the spectral characteristics of Landsat imagery and associated shortcomings, follow-up studies could incorporate very-high-resolution Earth observation technologies such as Unmanned Aerial Vehicle (UAV) drones to understand the current forms of land use changes and degradation along the critical zones of the park and its periphery.

5. Conclusions

This study investigated land cover changes using Landsat satellite images of 1978, 1988, 2001, 2010, and 2020 for the upper Manafwa watershed, at the slopes of Mount Elgon, Uganda, using supervised classification. In 1978, the dominant land cover classes (>10%) were tropical high forest well-stocked (43.64%), grassland (15.55%), and agriculture (10.63%). By 2020, the major land cover classes (>10%) included agriculture (30.43%), tropical high forest well-stocked (21.63%), and tropical high forest low-stocked (18.96%). Although there were several land cover transitions observed between 1978 and 2020, shrubs recorded the highest losses (99.51%), closely followed by bushland (98.26%), planted forest (96.38%), and tropical high forest low-stocked (91.08%). Agriculture and bare and sparsely vegetated surfaces recorded the lowest transitions to other classes (27.29% and 39.03%, respectively). The trend of land cover flows found in this study, especially the areas of deforestation and loss of natural vegetation cover, provides resourceful information for policy makers and responsible authorities to further take appropriate decisions and actions to revert the situation and reduce encroachment into the national park.

Landsat satellite images provide crucial information on change detection. Despite the emergence of new image classification methods such as SVM, the maximum likelihood method still provides reliable results. However, near-real-time monitoring systems of human disturbances in conservation areas and the use of very-high-resolution images should be incorporated by further studies to monitor changes and actions taken to minimize forest encroachment.

Supplementary Materials: The following supporting information can be downloaded at: https://www.mdpi.com/article/10.3390/rs14102423/s1, Figure S1: Aerial Photograph for the area around Bududa Town Council in 1960 (Source; Mapping and Surveys Department).

Author Contributions: Conceptualization, H.O., S.M., J.E.M.B. and F.M.; data curation, H.O.; formal analysis, H.O., S.M. and S.N.; funding acquisition, S.M., J.E.M.B. and F.M.; investigation, H.O.; methodology, H.O. and S.N.; resources, H.O., S.M., J.E.M.B. and F.M.; software, H.O., S.M. and S.N.; validation, H.O., S.M. and S.N.; visualization, H.O., S.M., J.E.M.B., S.N. and F.M.; writing—original draft, H.O.; and writing—review and editing, H.O., S.M., J.E.M.B., S.N. and F.M. All authors have read and agreed to the published version of the manuscript.

Funding: This study was conducted within the MWARES Project being implemented by a consortium of Africa 2000 Network—Uganda, Wageningen University & Research, Makerere University, Kyambogo University, and Tree Adoption Uganda with funding from Stichting DOB Ecology (5200044445).

Data Availability Statement: Remote sensing (Landsat satellite) data are available from the USGS (http://glovis.usgs.gov (accessed on 15 December 2020)) for free. For the moment, the rest of the data from the project are not available, due to restrictions.

Acknowledgments: We acknowledge support from Uganda Wildlife Authority and specifically the Mount Elgon Conservation Area leadership, Manafwa Watershed Restoration (MWARES) Project consortium members, and stakeholders from local community members in Bududa.

Conflicts of Interest: The authors declare no conflict of interest.

References

1. Geist, H.; Lambin, F.E. *Land Use and Land Cover Change: Local Processes and Global Impacts*; Springer: Berlin, Germany, 2006; ISBN 9783540322016.
2. Lillesand, T.M.; Kiefer, R.W.; Chipman, J.W. *Remote Sensing and Image Interpretation*, 7th ed.; John Wiley & Sons, Ltd.: Las Vegas, NV, USA, 2015; Volume 81, ISBN 9781118343289.
3. Turner, B.L., II; Lambin, E.F.; Verburg, P.H. From land-use/land-cover to land system science: This article belongs to Ambio's 50th Anniversary Collection. Theme: Agricultural land use. *AMBIO* **2021**, *50*, 1291–1294. [CrossRef] [PubMed]
4. Islam, K.; Jashimuddin, M.; Nath, B.; Nath, T.K. Land use classification and change detection by using multi-temporal remotely sensed imagery: The case of Chunati wildlife sanctuary, Bangladesh. *Egypt. J. Remote Sens. Sp. Sci.* **2018**, *21*, 37–47. [CrossRef]
5. Hailemariam, S.N.; Soromessa, T.; Teketay, D. Land Use and Land Cover Change in the Bale Mountain Eco-Region of Ethiopia during 1985 to 2015. *Land* **2016**, *5*, 41. [CrossRef]
6. MohanRajan, S.N.; Loganathan, A.; Manoharan, P. Survey on Land Use/Land Cover (LU/LC) change analysis in remote sensing and GIS environment: Techniques and Challenges. *Environ. Sci. Pollut. Res.* **2020**, *27*, 29900–29926. [CrossRef]
7. Prakasam, C. Land use and land cover change detection through remote sensing approach: A case study of Kodaikanal taluk, Tamil nadu. *Int. J. Geomat. Geosci.* **2010**, *1*, 150–158.
8. Maina, J.; Wandiga, S.; Gyampoh, B.; Charles, K. Assessment of Land Use and Land Cover Change Using GIS and Remote Sensing: A Case Study of Kieni, Central Kenya. *J. Remote Sens. GIS* **2020**, *9*, 1–5. [CrossRef]
9. Thakur, T.K.; Patel, D.K.; Bijalwan, A.; Dobriyal, M.J.; Kumar, A.; Thakur, A.; Bohra, A.; Bhat, J.A. Land use land cover change detection through geospatial analysis in an Indian Biosphere Reserve. *Trees For. People* **2020**, *2*, 100018. [CrossRef]
10. Alijani, Z.; Hosseinali, F.; Biswas, A. Spatio-temporal evolution of agricultural land use change drivers: A case study from Chalous region, Iran. *J. Environ. Manage.* **2020**, *262*, 110326. [CrossRef]
11. Geist, H.; McConnell, W.; Lambin, F.E.; Moran, E.; Alves, D.; Rudel, T. Causes and Trajectories of Land-Use/Cover Change. In *Land-Use and Land-Cover Change; Local Processes and Global Impacts*; Lambin, F.E., Geist, H., Eds.; Springer: Berlin, Germany, 2006; pp. 1–236. ISBN 3-540-32201-9.
12. Druga, M.; Falťan, V. Influences of Environmental Drivers on Land Cover Structure and its Long-Term Changes: A Case Study of the Villages of Malachov and Podkonice in Slovakia. *Morav. Geogr. Rep.* **2014**, *22*, 29–41. [CrossRef]
13. Lambin, E.F.; Turner, B.L.; Geist, H.J.; Agbola, S.B.; Angelsen, A.; Bruce, J.W.; Coomes, O.T.; Dirzo, R.; Fischer, G.; Folke, C.; et al. The causes of land-use and land-cover change: Moving beyond the myths. *Glob. Environ. Chang.* **2001**, *11*, 261–269. [CrossRef]
14. Geist, H.J.; Lambin, E.F. Proximate causes and underlying driving forces of tropical deforestation. *Bioscience* **2002**, *52*, 143–150. [CrossRef]
15. Kindu, M.; Schneider, T.; Teketay, D.; Knoke, T. Drivers of land use/land cover changes in Munessa-Shashemene landscape of the south-central highlands of Ethiopia. *Environ. Monit. Assess.* **2015**, *187*, 452. [CrossRef]
16. Kleemann, J.; Baysal, G.; Bulley, H.N.N.; Fürst, C. Assessing driving forces of land use and land cover change by a mixed-method approach in north-eastern Ghana, West Africa. *J. Environ. Manage.* **2017**, *196*, 411–442. [CrossRef]
17. Bekele, B.; Wu, W.; Yirsaw, E. Drivers of land use-land cover changes in the central rift valley of Ethiopia. *Sains Malays.* **2019**, *48*, 1333–1345. [CrossRef]
18. Petursson, J.G.; Vedeld, P.; Sassen, M. An institutional analysis of deforestation processes in protected areas: The case of the transboundary Mt. Elgon, Uganda and Kenya. *For. Policy Econ.* **2013**, *26*, 22–33. [CrossRef]
19. Kamwi, J.M.; Cho, M.A.; Kaetsch, C.; Manda, S.O.; Graz, F.P.; Chirwa, P.W. Assessing the spatial drivers of land use and land cover change in the protected and communal areas of the Zambezi Region, Namibia. *Land* **2018**, *7*, 131. [CrossRef]
20. Singh, A. Review Articlel: Digital change detection techniques using remotely-sensed data. *Int. J. Remote Sens.* **1989**, *10*, 989–1003. [CrossRef]
21. Vivekananda, G.N.; Swathi, R.; Sujith, A.V.L.N. Multi-temporal image analysis for LULC classification and change detection. *Eur. J. Remote Sens.* **2020**, *54*, 189–199. [CrossRef]
22. Berihun, M.L.; Tsunekawa, A.; Haregeweyn, N.; Meshesha, D.T.; Adgo, E.; Tsubo, M.; Masunaga, T.; Fenta, A.A.; Sultan, D.; Yibeltal, M. Exploring land use/land cover changes, drivers and their implications in contrasting agro-ecological environments of Ethiopia. *Land Use Policy* **2019**, *87*, 104052. [CrossRef]
23. Fichera, C.R.; Modica, G.; Pollino, M. Land Cover classification and change-detection analysis using multi-temporal remote sensed imagery and landscape metrics. *Eur. J. Remote Sens.* **2012**, *45*, 1–18. [CrossRef]
24. Cakir, H.I.; Khorram, S.; Nelson, S.A.C. Correspondence analysis for detecting land cover change. *Remote Sens. Environ.* **2006**, *102*, 306–317. [CrossRef]
25. Hoyos, L.E.; Cabido, M.R.; Cingolani, A.M. A multivariate approach to study drivers of land-cover changes through remote sensing in the dry Chaco of Argentina. *ISPRS Int. J. Geo-Inf.* **2018**, *7*, 170. [CrossRef]
26. Afify, H.A. Evaluation of change detection techniques for monitoring land-cover changes: A case study in new Burg El-Arab area. *Alex. Eng. J.* **2011**, *50*, 187–195. [CrossRef]
27. Forkuo, E.K.; Frimpong, A. Analysis of Forest Cover Change Detection. *Int. J. Remote Sens. Appl.* **2012**, *2*, 82–92.
28. Liu, S.; Su, H.; Cao, G.; Wang, S.; Guan, Q. Learning from data: A post classification method for annual land cover analysis in urban areas. *ISPRS J. Photogramm. Remote Sens.* **2019**, *154*, 202–215. [CrossRef]

29. Hishe, H.; Giday, K.; Van Orshoven, J.; Muys, B.; Taheri, F.; Azadi, H.; Feng, L.; Zamani, O.; Mirzaei, M.; Witlox, F. Analysis of Land Use Land Cover Dynamics and Driving Factors in Desa'a Forest in Northern Ethiopia. *Land Use Policy* **2020**, *101*, 105039. [CrossRef]
30. Qian, Y.; Zhou, W.; Yan, J.; Li, W.; Han, L. Comparing machine learning classifiers for object-based land cover classification using very high resolution imagery. *Remote Sens.* **2015**, *7*, 153–168. [CrossRef]
31. Karpatne, A.; Jiang, Z.; Raju Vatsavai, R.; Shekhar, S.; Kumar, V. Monitoring Land-Cover Changes: A machine-learning perspective. *IEEE Geosci. Remote Sens. Lett.* **2016**, *4*, 8–21. [CrossRef]
32. Uganda Wildlife Authority (UWA). *Mount Elgon National Park General Management Plan 2009–2019*; Uganda Wildlife Authority (UWA): Kampala, Uganda, 2009.
33. United Nations Environment Programme (UNEP). GEAS from hotspots to hopespots: Connecting local changes to global audiences. *Environ. Dev.* **2013**, *8*, 95–104. [CrossRef]
34. Uganda Bureau of Statistics (UBOS). *The National Population and Housing Census 2014, Area Specific Profile Series*; Uganda Bureau of Statistics (UBOS): Kampala, Uganda, 2017.
35. Nakileza, B.R. Rethinking the future of rural landscapes in relation to cities in the mountain regions of East Africa: Case of Mt Elgon in Uganda. In *Rural-Urban Dynamics in the East African Mountains*; Racaud, S., Nakileza, R.B., Bart, F., Eds.; Mkuki na Nyota Publishers: Dar es Salaam, Tanzania, 2016; pp. 91–112. ISBN 9782957305827.
36. Sassen, M.; Sheil, D.; Giller, K.E. Fuelwood collection and its impacts on a protected tropical mountain forest in Uganda. *For. Ecol. Manage.* **2015**, *354*, 56–67. [CrossRef]
37. Himmelfarb, D.; Cavanagh, C.J. Managing the contradictions: Conservation, communitarian rhetoric, and conflict at Mount Elgon National Park. In *Conservation and Development in Uganda*; Sandbrook, C., Cavanagh, C.J., Mwesigye, T.D., Eds.; Routledge: New York, NY, USA, 2018; pp. 85–103. ISBN 978-1-138-71092-4(hbk).
38. Hansen, M.C.; Potapov, P.V.; Moore, R.; Hancher, M.; Turubanova, S.A.; Tyukavina, A.; Thau, D.; Stehman, S.V.; Goetz, S.J.; Loveland, T.R.; et al. Global Deforestation Rates & Statistics by Country | GFW. Available online: http://www.globalforestwatch.org/dashboards/global/?category=summary&dashboardPrompts=eyJzaG93UHJvbXB0cyI6dHJ1ZSwicHJvbXB0c1ZpZXdlZCI6WyJ3aWRnZXRTZXR0aW5ncyJdLCJzZXR0aW5ncyI6eyJzaG93UHJvbXB0cyI6dHJ1ZSwicHJvbXB0c1ZpZXdlZCI6W10sInNldHRpbmdzIjp7Im9wZW4iOmZhb (accessed on 29 January 2021).
39. Mugagga, F.; Kakembo, V.; Buyinza, M. Land use changes on the slopes of Mount Elgon and the implications for the occurrence of landslides Catena Land use changes on the slopes of Mount Elgon and the implications for the occurrence of landslides. *Catena* **2012**, *90*, 39–46. [CrossRef]
40. Staudt, M.; Kuosmanen, E.; Babirye, P.; Lugaizi, I. *The Bududa landslide of 1 March 2010*; Geological Survey of Finland: Espoo, Finland, 2014; Volume 56.
41. Bunyangha, J.; Majaliwa, M.J.G.; Muthumbi, A.W.; Gichuki, N.N.; Egeru, A. Past and future land use/land cover changes from multi-temporal Landsat imagery in Mpologoma catchment, eastern Uganda. *Egypt. J. Remote Sens. Sp. Sci.* **2021**, *24*, 675–685. [CrossRef]
42. Broeckx, J.; Maertens, M.; Isabirye, M.; Vanmaercke, M.; Namazzi, B.; Deckers, J.; Tamale, J.; Jacobs, L.; Thiery, W.; Kervyn, M.; et al. Landslide susceptibility and mobilization rates in the Mount Elgon region, Uganda. *Landslides* **2019**, *16*, 571–584. [CrossRef]
43. Bamutaze, Y.; Mukwaya, P.; Oyama, S.; Nadhomi, D.; Nsemire, P. Intersecting RUSLE modelled and farmers perceived soil erosion risk in the conservation domain on mountain Elgon in Uganda. *Appl. Geogr.* **2021**, *126*, 102366. [CrossRef]
44. Wanyama, D.; Moore, N.J.; Dahlin, K.M. Persistent vegetation greening and browning trends related to natural and human activities in the mount Elgon ecosystem. *Remote Sens.* **2020**, *12*, 2113. [CrossRef]
45. Mugagga, F.; Nagasha, B.; Barasa, B.; Buyinza, M. The Effect of Land Use on Carbon Stocks and Implications for Climate Variability on the Slopes of Mount Elgon, Eastern Uganda. *Int. J. Reg. Dev.* **2015**, *2*, 58. [CrossRef]
46. Scott, P. *From Conflict to Collaboration: People and Forests at Mount Elgon, Uganda*; IUCN: Gland, Switzerland; Cambridge, UK, 1998; ISBN 2831703859.
47. Vlaeminck, P.; Maertens, M.; Isabirye, M.; Vanderhoydonks, F.; Poesen, J.; Deckers, S.; Vranken, L. Coping with landslide risk through preventive resettlement. Designing optimal strategies through choice experiments for the Mount Elgon region, Uganda. *Land Use Policy* **2016**, *51*, 301–311. [CrossRef]
48. Jiang, B.; Bamutaze, Y.; Pilesjö, P. Climate change and land degradation in Africa: A case study in the Mount Elgon region, Uganda. *Geo-Spat. Inf. Sci.* **2014**, *17*, 39–53. [CrossRef]
49. Bagoora, F.D.K. Soil Erosion and Mass Wasting Risk in the Highland Area of Uganda. *Mt. Res. Dev.* **1988**, *8*, 173–182. [CrossRef]
50. Kitutu, M.G. Land Slide Occurences in the Hilly Areas of Bududa District and Their Causes. Ph.D. Thesis, Makerere University, Kampala, Uganda, 2010.
51. Claessens, L.; Knapen, A.; Kitutu, M.G.; Poesen, J.; Deckers, J.A. Modelling landslide hazard, soil redistribution and sediment yield of landslides on the Ugandan footslopes of Mount Elgon. *Geomorphology* **2007**, *90*, 23–35. [CrossRef]
52. Mugagga, F. *Landuse Change, Landslide Occurrence and Livilihood Strategies on Mount Elgon Slopes, Eastern Uganda*; Nelson Metropolitan University: Gqeberha, South Africa, 2011; Volume 11.
53. Bamutaze, Y.; Tenywa, M.M.; Majaliwa, M.J.G.; Vanacker, V.; Bagoora, F.; Magunda, M.; Obando, J.; Wasige, J.E. Infiltration characteristics of volcanic sloping soils on Mt. Elgon, Eastern Uganda. *CATENA* **2010**, *80*, 122–130. [CrossRef]

54. Bududa, D.L.G. *Bududa District Local Government: Five-Year District Development Plan 2010/11 to 2014/15*; National Planning Authority: Kampala, Uganda, 2010.
55. Showstack, R. Landsat 9 Satellite Continues Half-Century of Earth Observations. *Bioscience* **2022**, *72*, 226–232. [CrossRef]
56. Yang, Y.; Erskine, P.D.; Lechner, A.M.; Mulligan, D.; Zhang, S.; Wang, Z. Detecting the dynamics of vegetation disturbance and recovery in surface mining area via Landsat imagery and LandTrendr algorithm. *J. Clean. Prod.* **2018**, *178*, 353–362. [CrossRef]
57. Forkuor, G.; Dimobe, K.; Serme, I.; Tondoh, J.E. Landsat-8 vs. Sentinel-2: Examining the added value of sentinel-2's red-edge bands to land-use and land-cover mapping in Burkina Faso. *GISci. Remote Sens.* **2018**, *55*, 331–354. [CrossRef]
58. Alawadi, F. Detection of surface algal blooms using the newly developed algorithm surface algal bloom index (SABI). In *Remote Sensing of the Ocean, Sea Ice, and Large Water Regions 2010*; International Society for Optics and Photonics: Bellingham, WA, USA, 2010; Volume 7825, p. 782506.
59. Food and Agriculture Organization (FAO). *Land Cover Classification System—Classification Concepts and Software Version 3*; FAO: Rome, Italy, 2016; ISBN 978-92-5-109017-6.
60. Anderson, J.R.; Hardy, E.E.; Roach, J.T.; Witmer, R.E. A Land Use and Land Cover Classification System for Us with Remote Sensor Data. In *Geological Survey Professional Paper*; U.S Printing Office: Washington, DC, USA, 1983; p. 964.
61. National Forestry Authority. *National Biomass Study*; Technical Report 2009; NFA: Kampala, Uganda, 2009; p. 109.
62. Phiri, D.; Simwanda, M.; Salekin, S.; Nyirenda, V.R.; Murayama, Y.; Ranagalage, M. remote sensing Sentinel-2 Data for Land Cover/Use Mapping: A Review. *Remote Sens.* **2020**, *12*, 2291. [CrossRef]
63. Olofsson, P.; Foody, G.M.; Stehman, S.V.; Woodcock, C.E. Making better use of accuracy data in land change studies: Estimating accuracy and area and quantifying uncertainty using stratified estimation. *Remote Sens. Environ.* **2013**, *129*, 122–131. [CrossRef]
64. Olofsson, P.; Foody, G.M.; Herold, M.; Stehman, S.V.; Woodcock, C.E.; Wulder, M.A. Good practices for estimating area and assessing accuracy of land change. *Remote Sens. Environ.* **2014**, *148*, 42–57. [CrossRef]
65. Tewkesbury, A.P.; Comber, A.J.; Tate, N.J.; Lamb, A.; Fisher, P.F. A critical synthesis of remotely sensed optical image change detection techniques. *Remote Sens. Environ.* **2015**, *160*, 1–14.
66. Alawamy, J.S.; Balasundram, S.K.; Hanif, A.H.M.; Sung, C.T.B. Detecting and analyzing land use and land cover changes in the Region of Al-Jabal Al-Akhdar, Libya using time-series landsat data from 1985 to 2017. *Sustainability* **2020**, *12*, 4490. [CrossRef]
67. Gerard, F.; Petit, S.; Smith, G.; Thomson, A.; Brown, N.; Manchester, S.; Wadsworth, R.; Bugar, G.; Halada, L.; Bezák, P.; et al. Land cover change in Europe between 1950 and 2000 determined employing aerial photography. *Prog. Phys. Geogr.* **2010**, *34*, 183–205. [CrossRef]
68. Sassen, M.; Sheil, D.; Giller, K.E.; Braak, C.J.F. ter Complex contexts and dynamic drivers: Understanding four decades of forest loss and recovery in an East African protected area. *Biol. Conserv.* **2013**, *159*, 257–268. [CrossRef]
69. National Forestry Authority (NFA). *Gazetted Areas GIS Database*; National Forestry Authority (NFA): Kampala, Uganda, 2007.
70. Pontius, R.G.G. Quantification error versus location error in comparison of categorical maps. *Photogrametric Eng. Remote Sens.* **2000**, *66*, 1011–1016.
71. Sousa, S.; Caeiro, S.; Painho, M. Assessment of map similarity of categorical maps using kappa statistics; The Case of Sado Estuary. *ISEGI* **2002**, *2*, 2–7.
72. Hailu, A.; Mammo, S.; Kidane, M. Dynamics of land use, land cover change trend and its drivers in Jimma Geneti District, Western Ethiopia. *Land Use Policy* **2020**, *99*, 105011. [CrossRef]
73. Masaba, S.; Mungai, D.N.; Isabirye, M.; Nsubuga, H. Implementation of landslide disaster risk reduction policy in Uganda. *Int. J. Disaster Risk Reduct.* **2017**, *24*, 326–331. [CrossRef]
74. Alam, A.; Bhat, M.S.; Maheen, M. Using Landsat satellite data for assessing the land use and land cover change in Kashmir valley. *GeoJournal* **2019**, *85*, 1529–1543. [CrossRef]
75. Bantider, A.; Hurni, H.; Zeleke, G. Responses of rural households to the impacts of population and land-use changes along the Eastern Escarpment of Wello, Ethiopia. *Nor. J. Geogr.* **2011**, *65*, 42–53. [CrossRef]
76. Liu, C.; Li, W.; Zhu, G.; Zhou, H.; Yan, H.; Xue, P. Land use/land cover changes and their driving factors in the northeastern tibetan plateau based on geographical detectors and google earth engine: A case study in gannan prefecture. *Remote Sens.* **2020**, *12*, 3139. [CrossRef]
77. Nakakaawa, C.; Moll, R.; Vedeld, P.; Sjaastad, E.; Cavanagh, J. Collaborative resource management and rural livelihoods around protected areas: A case study of Mount Elgon National Park, Uganda. *For. Policy Econ.* **2015**, *57*, 1–11. [CrossRef]
78. Norgrove, L.; Hulme, D. Confronting conservation at Mount Elgon, Uganda. *Dev. Chang.* **2006**, *37*, 1093–1116. [CrossRef]
79. Medard, C. 'Indigenous' land claims in Kenya: A case study of Chebyuk, Mount Elgon District. In *The Struggle over Land in Africa: Conflicts, Politics and Change*; Answeeuw, W., Alden, C., Eds.; Human Sciences Research Council: Cape Town, South Africa, 2010; ISBN 9780796923226.
80. Himmelfarb, D. Moving people, moving boundaries: The socio-economic effects of protectionist conservation, involuntary resettlement and tenure insecurity on the edge of Mt. *Elgon National Park. Agrofor. Landsc. Mosaics* **2006**, *7*, 13.
81. Shaban, K.S.; Okumu, J.O.; Paul, O.; Joseph, O. Assessing community-based organizations' influence on trees and grass planting for forest, soil and water management around Mt. *Elgon National Park in Uganda. For. Trees Livelihoods* **2016**, *25*, 161–172. [CrossRef]
82. Buyinza, J.; Nuberg, K.I.; Muthuri, W.C.; Denton, D.M. Farmers' Knowledge and Perceptions of Management and the Impact of Trees on Farm in the Mt. Elgon Region. *Small-Scale For.* **2021**, *21*, 71–92. [CrossRef]

83. Båtvik, S.T.; Kaboggoza, J.R.S.; Kabutha, C.; Vedeld, P. *Mount Elgon Regional Ecosystem Conservation Programme (MERECP): Appraisal Report*; Noragric, Centre for International Environment and Development Studies: Ås, Norway, 2002.
84. Muhweezi, A.B.; Sikoyo, G.M.; Chemonges, M.M. Introducing a Transboundary Ecosystem Management Approach in the Mount Elgon Region: The need for strengthened institutional collaboration. *Mt. Res. Dev.* **2007**, *27*, 215–219. [CrossRef]
85. FAO; UNEP. *The State of World's Forests 2020: Forests, Biodiversity and People*; FAO: Rome, Italy, 2020.
86. Kessler, C.A.; van Duivenbooden, N.; Nsabimana, F.; van Beek, C.L. Bringing ISFM to scale through an integrated farm planning approach: A case study from Burundi. *Nutr. Cycl. Agroecosyst.* **2016**, *105*, 249–261. [CrossRef]
87. Buyinza, J.; Nuberg, I.K.; Muthuri, C.W.; Denton, M.D. Assessing smallholder farmers' motivation to adopt agroforestry using a multi-group structural equation modeling approach. *Agrofor. Syst.* **2020**, *94*, 2199–2211. [CrossRef]